AIAA 80-0430R

Simulation and Modeling of Jet Plumes in Wind Tunnel Facilities

H.H. Korst* and R.A. White†
University of Illinois at Urbana-Champaign, Urbana, Ill.
and
S.-E. Nyberg‡, and J. Agrell§
The Aeronautical Research Institute of Sweden, Bromma, Sweden

A high-pressure hot gas supply system has been developed for the FFA 0.5 × 0.5-m supersonic wind tunnel to allow the study of aerodynamic interference effects caused by plume-induced flow separation from propulsive afterbodies. Capable of operating with a variety of gases covering a wide range of specific heat ratios, the facility serves to evaluate the merits and potential of a new plume simulation methodology based on second-order geometrical modeling schemes which are required for cases involving large near wake dimensions. Experimental programs carried out with air and Freon-22 confirmed the correctness of the theory with the accuracy of modeling extending over wide ranges of jet-to-ambient pressure ratios straddling the design point. Beyond the ability to correctly model and interpret near wake pressures and slip-stream separation locations, the new methodology allows experiments with diatomic inert gases (air or N_2, $\gamma = 1.4$) at much lower stagnation pressures than would be required for propellants of lower specific heat ratios.

Nomenclature

Geometry

Afterbody

D = forebody diameter (m)
L = boattail length (m)
α = angle of attack (deg)
β = boattail angle (deg)

Nozzle

R_L = exit or lip radius (m)
R^* = throat radius (m)
R_c^* = radius of throat wall curvature (m)
θ_L = conical divergence angle (deg)

Tunnel flow

p_{0E} = stagnation pressure (MPa)
p_E = freestream static presssure (MPa)
M_E = freestream Mach No. (−)

Nozzle flow

M_L = lip Mach No. (−)¶
p_{0I} = nozzle stagnation pressure (MPa)
p_L = lip pressure (MPa)
T_{0I} = nozzle stagnation temperature (°C)
γ = specific heat ratio [−]
ω_L = Prandtl-Meyer angle corresponding to M_L (deg)

Plume

M^* = critical Mach No. [−]
M_F = surface Mach No. [−]
R_c = initial surface curvature (m)
r_c = R_c/R_L [−]
θ_F = initial surface slope (deg.)
ω_F = Prandtl-Meyer angle corresponding to M_F (deg)

Wake conditions

p_b = wake (base) pressure (MPa)
s = separation distance measured from end of boattail (m)

Subscripts

A = air
F = Freon
M = model
P = prototype

Presented as Paper 80-0430 at the AIAA 11th Aerodynamic Testing Conference, Colorado Springs, Colo., March 18-20, 1980; submitted March 18, 1980; revision received March 27, 1981.

*Professor of Mechanical Engineering. Fellow AIAA.
†Professor of Mechanical Engineering.
‡Director, Aeronautic Dept., Retired, and Consultant to FFA.
§Senior Research Scientist, FFA.

¶Conical source flow assumed, otherwise nozzle geometry and lip conditions have to be specified in greater detail, see Ref. 13.

I. Introduction

THE interaction of rocket or jet plumes with the external flow over a vehicle as well as surrounding equipment or surfaces is important to system performance.[1] In particular, such interactions are critical in their effects on the near wake base temperature and pressure, flow over the vehicle itself in case of external flow separation, wake flowfield at angle of attack, afterbody fin effectiveness, and launch equipment performance. Thus, the jet/slip-stream interactions can give rise to undesirable aerodynamic performance by introducing drag penalties through lower than ambient pressures or, as the ratio of jet stagnation pressure to ambient pressure increases, by leading to plume-induced separation.[2] A typical flow configuration involving plume-induced separation from a conical afterbody, identifying geometrical and operational parameters, is shown in Fig. 1. In extreme cases, plume-induced separation can result in catastrophic pitch-up of missiles because of loss of stability or degradation of control effectiveness.[3]

Rocket or jet plumes have been generated in wind tunnel tests using a variety of methods which include the use of cold or heated air through geometrically modeled nozzles, small rocket motors, and solid bodies which simulate the plume shape (either calculated or determined from Schlieren photographs of jet plumes). Shortcomings inherent in these methods can be traced to failure to account for all, or part, of such factors as plume deflection, mass entrainment, wake

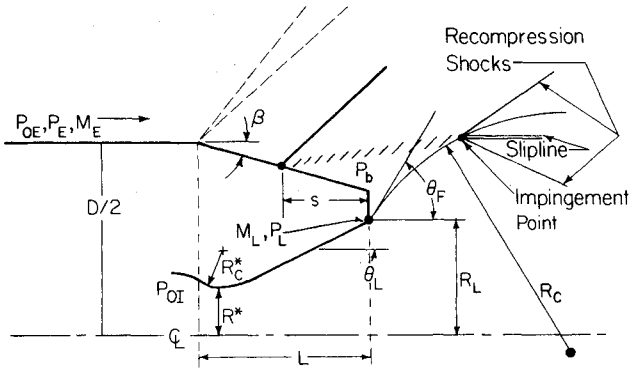

Fig. 1 Flow configuration for plume-induced separation from conical afterbody (geometrical and operational parameters identified).

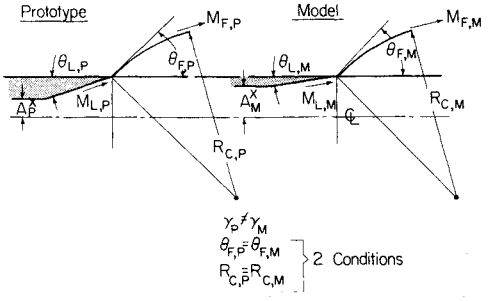

Fig. 2 Schematic of geometrical plume modeling (Ref. 13).

closure, influence of specific heat ratio, viscous effects, geometry, and temperature. It is, of course, impossible to take account of all the contributing parameters simultaneously in a simulation test and such difficulties are pointed to in a recent NASA technical paper.[4]

Further, simulation by specified gases may become necessary due to wind tunnel operating environments. An excellent example is the National Transonic Facility (NTF) for which one of the recommendations of the panel on propulsion aerodynamics[5] states: "An extensive research program is needed to determine and validate jet simulation techniques for the special conditions encountered in the NTF.**

While some methods of plume simulation appear to be more appropriate than others, i.e., cold gas rather than solid surfaces, only limited comparisons have been undertaken between results for simulation models and actual prototypes. In addition, documentation of the importance of individual factors such as plume geometry, plume stiffness (i.e., jet surface Mach number), and wake closure conditions for the various Mach number regimes has been lacking, although strictly empirical correlations have been suggested†† for space shuttle applications. This paper utilizes an analytical basis for proper plume modeling in wind tunnels, describes a new facility constructed to examine and compare the merits of jet simulation modeling schemes, and presents information to clarify the roles of various parameters on the simulation of jets and their interaction with the slip-stream and surrounding equipment.

II. Methodology

Integral and component approaches to near wake solutions, with their wake closure conditions linked to second law concepts, have led to a basic understanding of the problem and even to the establishment of relations[6] accounting, in principle, for the influence of all pertinent variables. The difficulty of making specific assessments concerning the wake closure has led to extensive experimental studies in support of semiempirical relations to account for the incomplete realignment of streamlines during recompression.[7]

Experimental programs require proper plume simulation whenever the use of prototype propellants is not feasible. The modeling of plume interactions requires, in principle, geometrically congruent inviscid jet contours and correct pressure rise-jet boundary deflection (plume stiffness) as well as mass entrainment characteristics along the wake boundaries. Thus, modeling with gaseous plumes is needed and normally involves dissimilar specific heat ratios.

The importance of generating the correct jet plume geometry has been stressed in prior efforts to establish modeling laws between propellant gases having dissimilar specific heat ratios.[8-10] However, the geometrical requirements were only formulated for the initial deflection angle of the jet, a condition not stringent enough to cope with plume-induced separation.[8]

A second-order approximation for dealing with axisymmetric centered expansions[11] forms the basis for geometrical jet plume surface modeling in this study.[12] This approach allows the matching of not only the initial deflection angle but also the plume radius of curvature (shape), see Fig. 2. It can be shown that the accuracy attained by such a procedure extends well beyond the range of convergence for the corner expansion itself.[13]

The plume expansion derives its initial conditions from the flow approaching the end of the nozzle. For the case where exit conditions can be sufficiently well described, locally, by conical source flow (M_L, θ_L), sweeping simplifications in the interpretation of results are possible.[13] The solutions lead to a direct correspondence of nozzle shapes producing the same plume boundary geometry with one free parameter remaining available for satisfying the recompression conditions at the end of the separated flow region. It is thus possible to determine nozzle exit conditions in terms of Mach number at the nozzle lip and the nozzle divergence angle at the lip which will geometrically duplicate the jet contour produced by a gas with a different specific heat ratio as it expands from a given nozzle under specified adjacent conditions (within the present degree of approximation), that is,

$$\theta_{F,M} = \theta_{F,P} \quad \text{and} \quad r_{C,M} = r_{C,P} \tag{1}$$

where the geometry and notation are shown in Fig. 2 and subscripts M and P are for model and prototype, respectively. The downstream specifying condition should properly account for the viscid aspects of the wake flow problem in their interaction with the inviscid components. With only one choice available as a result of the geometric requirements, it is obvious that one has to account, above all, for the proper pressure rise in the external flow.[8] The recompression mechanism of the dissipative boundary of the jet, as a consequence of its mass entrainment characteristics, will, however, generally not be simultaneously satisfied. While this effect may be expected to be small for cases involving strongly underexpanded plumes,[13] it is possible to account for it, in principle, by introducing mass bleed. The concept of equivalent mass bleed has been shown[7] to be useful for both mass and temperature effect simulations.

The well-documented[14] effect of plume stiffness has been examined in more detail in recent tests carried out at Calspan[15] using air nozzles designed according to the present method to produce a given plume geometry but with different jet surface Mach numbers. A wooden form of the same shape as the air plumes was also tested. The tests were carried out at subsonic, transonic, and supersonic external Mach numbers. General observations concerning the relative importance of simulation concepts resulting from these tests are summarized in Table 1. Related tests have also been carried out by the Aeronautical Research Institute of Sweden (FFA). Figure 3

**The NTF will be operated with cryogenic pure N_2.

††Oral communication from J.L. Sims, Marshall Space Flight Center.

Table 1 Current simulation concepts and experimental verification studies

Freestream Mach No.	Primary simulation concepts[a] (a) Geometry of plume	(b) Jet surface Mach No. (pliability)	(c) Ratio of specific heats	
$M<1$	Dominates	Apparently not significant	Important	
$M\simeq 1$ (transonic)	Important	Attains increasing significance	Important	
$M>1$	Important	Important	Important	
		Verification by wind tunnel tests		
Freestream Mach No.	FFA (ERO)	Calspan (MICOM)	Langley	AEDC
$M<1$		$x_{a,b}$		
$M\simeq 1$ (transonic)		$x_{a,b}$		x_c, planned
$M>1$	$x_{a,b,c}$		$x_{a,b}$	

[a] Secondary simulation concepts such as mass entrainment and streamline recompression may require attention but can be evaluated and accounted for using the concept of equivalent bleed.[7]

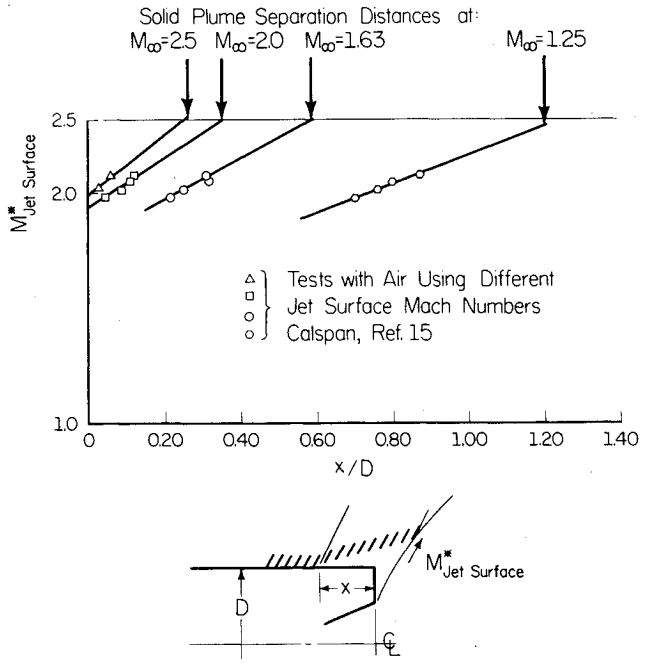

Fig. 3 Effect of plume stiffness (M_F) on separation distance for geometrically congruent plumes.

shows the effect of jet surface Mach number on plume-induced separation length for these tests. Use of critical Mach number, M^*, in Fig. 3 reflects the convenience of representing the case for infinite stiffness ($M_F\to\infty$) by a finite value of the abscissa $M^*\to[(\gamma+1)/(\gamma-1)]^{1/2}$ which, for $\gamma=1.40$, equals 2.4495. The results underscore the importance of the selection of plume flexibility characteristics to the simulation process particularly at supersonic Mach numbers. It is of interest to note that the separation distance induced by the wooden jet form correlates well with the air plume jet surface Mach numbers as one extrapolates to the limit for $M_F\to\infty$ corresponding to a rigid plume. Plume stiffness, therefore, must be properly identified. This is done by selecting the linearized (weak shock) approximation for the pressure rise streamline deflection relation:

$$[\gamma_M M_{F,M}^2/(M_{F,M}^2-1)^{1/2}]=[\gamma_P M_{F,P}^2/(M_{F,P}^2-1)^{1/2}] \quad (2)$$

With the primary and secondary simulation concepts stated (see Table 1), it is now necessary to identify the type of separation phenomenon to be investigated in order to establish design criteria for proper modeling.

For a known pressure distribution over the prototype afterbody due to the nonseparated slip-stream, one can estimate the pressure rise due to separation by utilizing information on free interactions[7] or slight modifications thereof due to local pressure gradients and/or surface slope discontinuities.[16] The resulting plateau pressure determines the jet surface Mach number $M_{F,P}$ so that the prototype conditions (nozzle flow, $M_{L,P}\theta_{L,P}$ especially for conical source flow) are all given and the model nozzle exit conditions $M_{L,M}\theta_{L,M}$ as well as the model jet surface Mach number $M_{F,M}$ [Eq. (2)] are determined.[12] Thus, for this "design point," Eqs. (1) and (2), will be satisfied.

In the vicinity of this design point, only the more stringent condition of the plume slope matching is retained. This can be expressed in the form

$$\theta_{F,M}=\theta_{F,P} \quad (3)$$

and

$$\omega_{F,P}=\theta_{L,M}-\theta_{L,P}+\omega_{L,P}-\omega_{L,M}+\omega_{F,M} \quad (4)$$

Since the nozzle flows—and therefore $\theta_{L,M}$, $\theta_{L,P}$, $\omega_{L,M}$, $\omega_{L,P}$—remain identical for design and off-design operation, one expects that the wake pressure ratios shall still be closely modeled; hence

$$p_b/p_E\,|_P=(p_b/p_E)_M=f(P_{0I,M}/P_{0E}) \quad (5)$$

Thus, one finds the pressure ratio for the prototype flow from the Prandtl-Meyer relation

$$M_{F,P}=f(\gamma_P,\omega_{F,P}) \quad (6)$$

and the identity

$$P_{0I,P}/p_{0E}=(P_{0I,P}/p_b)_{M_{F,P}}(p_b/p_E)_M \quad (7)$$

Consequently, for each model flow experiment series for which the relation

$$(p_b/p_E)_M=f[M_E,(p_{0I,M}/p_{0E}),\gamma_M] \quad (8)$$

has been established, the corresponding operating condition of the prototype flow can be determined.

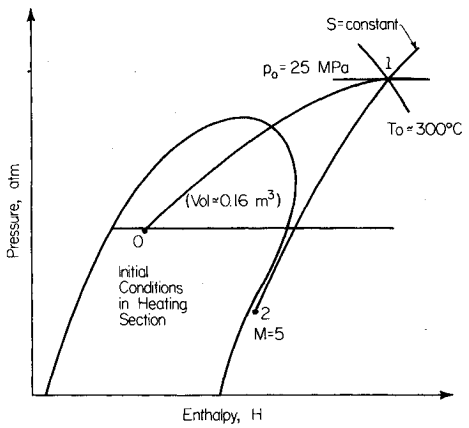

Fig. 4 Freon-22 simplified pressure enthalpy diagram with the schematic of thermodynamic process of heating at constant volume (heater) followed by isentropic expansion (nozzle).

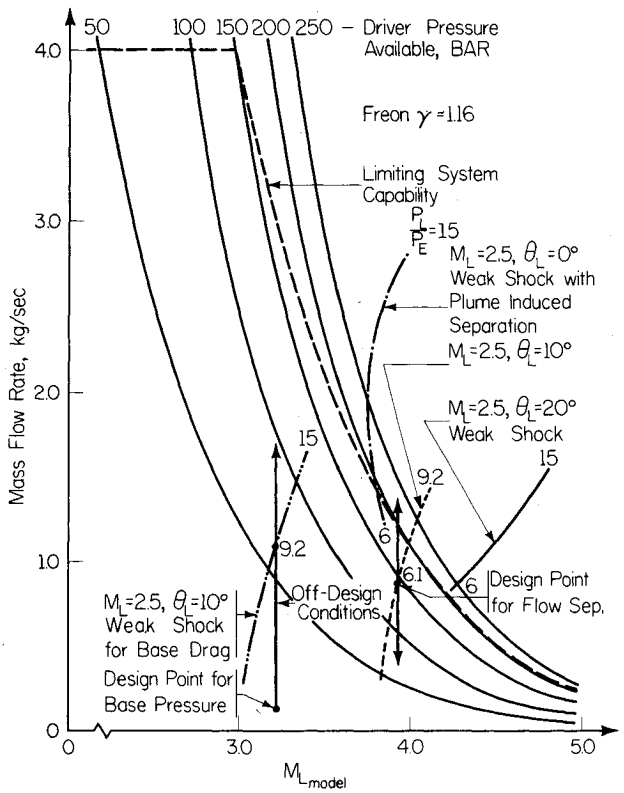

Fig. 5 Systems performance diagram showing operating conditions for initial model tests (see Fig. 10 for nozzle geometries, air nozzle, prototype, and design points selected).

III. Simulation Test Facility

A jet simulation test facility has been designed and constructed for use with the FFA 0.25-m^2 and 1.0-m^2 wind tunnels.[17] This unit has been developed with the objective of not only allowing wind tunnel jet experimentation with gases of various specific heat ratios but also to evaluate the modeling procedure specifying conditions outlined in Sec. II. Thus, it will be possible to critically evaluate the merits and limits of the analytical modeling procedures outlined. For this purpose, it is essential to have accurate test results and well-controlled operating conditions for both prototype and model. The test conditions should be well known in terms of the wind tunnel slip-stream flow and allow for careful control of the modeled propulsive jet, influence of transonic throat flow, nozzle design methodology, and working fluid. To this end, the design concept draws on the extensive test program

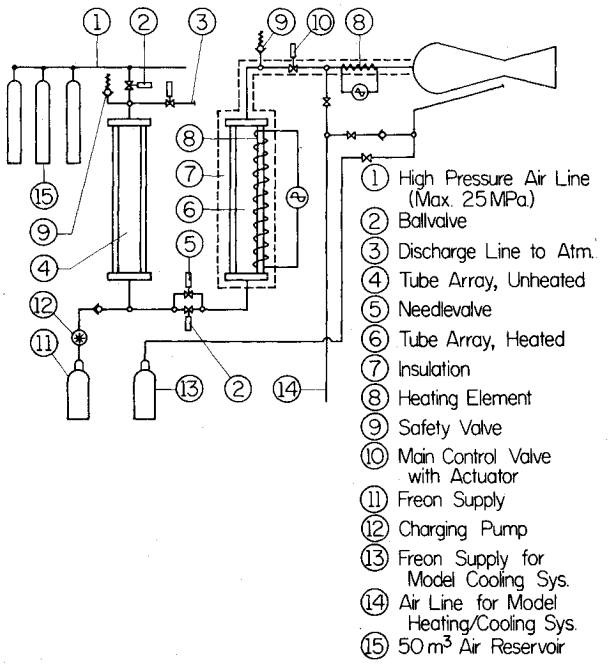

Fig. 6 Annotated schematic of air driver system, Freon heater, and nozzle.

on missile afterbody-jet performance which the FFA has carried out and reported on over the last 10 years.[16,18,19] This approach provides a wide base of well-documented results to be used as prototypes as well as allowing the utilization of a considerable portion of existing wind tunnel models and supporting equipment. The latter, in addition to reducing cost, guarantees that such factors as external boundary layer thickness remain largely unchanged in prototype or modeled configurations.

The selection of the test gas was based on availability, cost, nontoxicity, and having an appropriate ratio of specific heats without serious real gas effects. Various types of Freon have been used by other investigators[20] and consequently were among the obvious candidates. After an examination of alternatives, Freon-22 was chosen. Cost and chemical stability—which allows it to be heated to sufficiently high temperatures without chemical breakdown—were major factors in its selection. The latter should allow the expansion process to proceed to approximately Mach number 5 without crossing the condensation line. Figure 4 shows a simplified pressure-enthalpy diagram for Freon-22 illustrating the thermodynamic path for the Freon heating and nozzle expansion process. The ratio of specific heats at nozzle exit and plume expansion conditions, γ_F, is in the range of 1.16 to 1.18 which is appropriate for simulation of combustion-type jet products.

The modeled nozzles and their mass flow requirements based on configuration run with air in the previous FFA programs[16,18,19] (Prototype) were computed using the modeling procedures discussed in Sec. II. Shown in Fig. 5 is a systems performance diagram having the nozzle exit (lip) Mach number as abscissa, the nozzle mass flow rate as ordinate, and driver pressure level as a parameter. Mapped into this diagram are the operating conditions required for the modeling scheme. The nozzle configurations in the higher lip Mach number range (greater than approximately 4) require impractically high levels of pressure but, fortunately, are physically unrealistic as models since the nozzle divergence angles are generally excessive (greater than 40 deg half-angle).

The basic system makes use of the high-pressure storage of the FFAs hypersonic facilities[17] which allows the storage of 50 m^3 of air at a pressure of 25 MPa and is utilized in the simulation system as an essentially constant pressure driver for the Freon. Figure 6 is an annotated schematic of the Freon

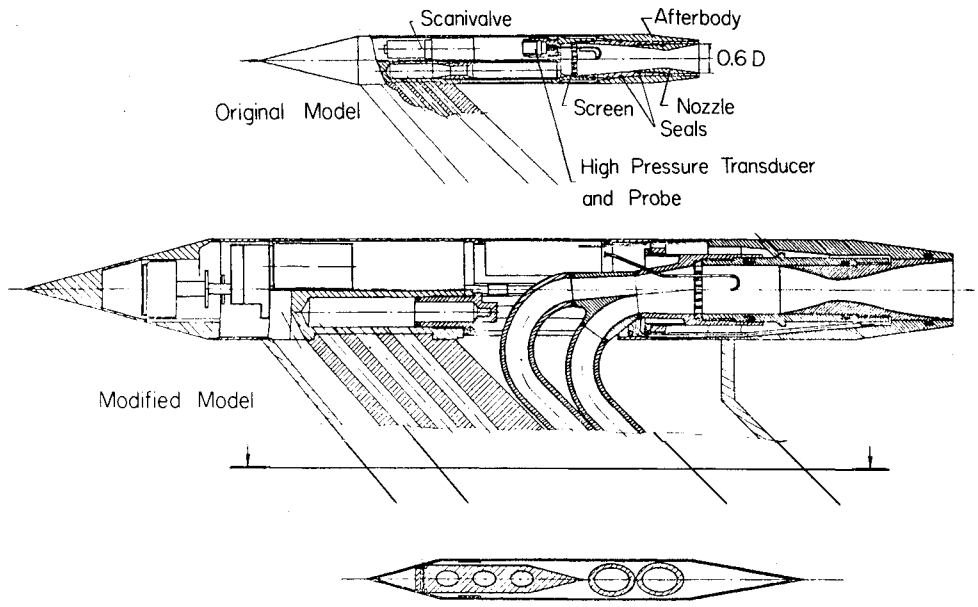

Fig. 7 Adaptation of propulsive afterbody wind tunnel model for operation with Freon.

system, the test model, and the high-pressure driver. Details of component design, construction, and operating procedures are given in Ref. 21 along with a discussion of the temperature control requirements and system developed for this purpose.

The facility consists of two parts: the unheated driver section and the heated and insulated section containing the test gas. Referring to the schematic (Fig. 6), the unheated pressure section and the heated and insulated part are constructed in a similar manner using vertical arrays of high-pressure tubes. The thermodynamic paths followed by the test gas are shown in Fig. 4 and consist of a constant volume heating process from points 0 to 1 and the essentially isentropic expansion through the nozzle from 1 to 2. The system is designed to provide the maximum supply capacity indicated (dashed line) in Fig. 5 with the upper limit determined by choking and the varying pressure line established by the maximum driving pressure and flow rate—pressure loss characteristics of the entire system. It can be seen in Fig. 5 that the design points of the selected simulation nozzles fall within the system operating range while allowing considerable off-design testing.

The basic design concepts of the system can best be illustrated by a brief discussion of the operational procedure. Prior to a run, the system is charged by the charging pump to the state where the heated portion contains the correct amount of Freon to reach the desired pressure and temperature after being heated at constant volume, that is, process 0-1 shown in Fig. 4. The required volume for the system described is approximately 0.16 m^3. The determination of the amount of Freon charged is facilitated by use of a pump revolution counter serving for metering purposes.

The hot and cold portions are now isolated and charging is continued until the unheated portion of the system has reached the pressure prescribed for the run (state 1 in Fig. 4). Small pressure corrections may be necessary and these can be made using either the needle valve, discharge line, or the charging pump as may be appropriate.

The heating process is accomplished by heating only a portion of the tubes, thus producing thermal circulation within the high-temperature tube array. The convection persists until the desired temperature is reached.

During a run, the cold Freon serves as a cushion between the air and test gas to prevent mixing of the driver air and hot test gas. The density relations between the cold Freon cushion and hot gas are such that thermal convection at the interface is inhibited.

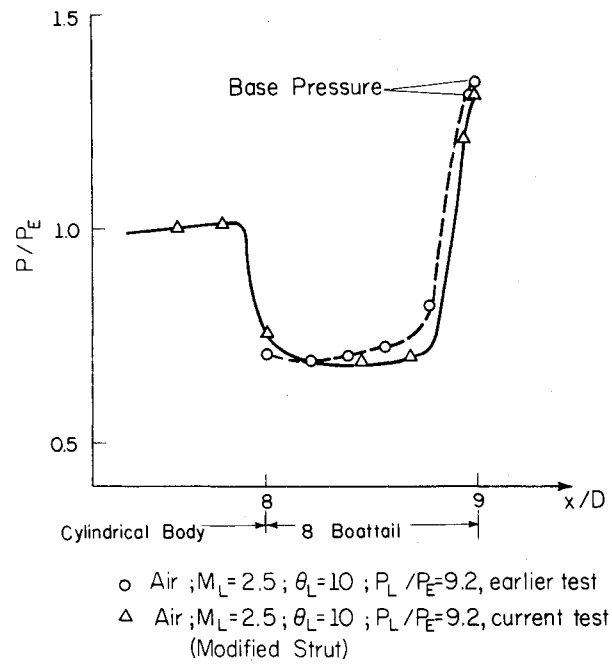

Fig. 8 Pressure distribution on the rear part of the body $M_F = 2.0$, $\alpha = 0$; effect of redesigned strut (five-digit numbers identify runs).

An individual run may last as long as the gas temperature remains constant (the system design is for 15-s test times). A small portion of the cold Freon will be sufficiently heated by entering and traversing the warm tube array to also serve as test gas and thus allowing slightly increased run times over the nominal design value. The latter has been found to contribute to pressure variations during a typical run as will be pointed out in the discussion of experimental results.

IV. Experimental Program

The compatibility of the Freon plume facility with the models reported on by the FFA in their basic jet interaction series of experiments provides a base of well-defined prototype conditions to be modeled while furnishing the information necessary to critically evaluate the accuracy and applicability of the plume simulation methodology discussed in Sec. II.

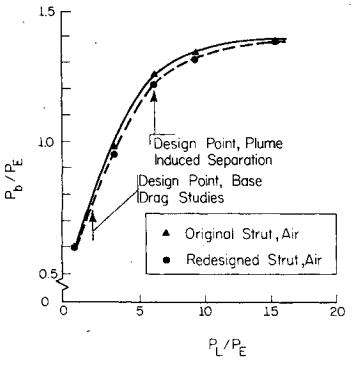

Fig. 9 Wake pressure ratio vs p_L/p_E for the air prototype nozzle showing effect of strut modification.

Wind Tunnel Models

The strut-supported wind tunnel model for the study of slip-stream plume interference effects used in the prototype air series[18] had to be modified to allow the heated high-pressure Freon to be introduced into the model with acceptable pressure losses. The latter requirement is important since modeling from air as prototype, to Freon, as model, requires higher pressure ratios.

Figure 7 shows both the original configuration and the modified version of the model. The additional Freon piping and its fairing increases the interference of the strut on the model afterbody flowfield. While the earlier strut configuration produced only negligible interference effects as has been confirmed by comparison with sting mounted runs, the new, enlarged fairing led to small but measurable differences in afterbody pressure distributions as shown in Fig. 8.

The small differences noted for the prototype pressure distribution due to the modified strut required that the air prototype tests be repeated over the range reported in earlier publications to guarantee that strut effects did not introduce unanticipated changes. The results from the current air tests are shown in Fig. 9. The results from the earlier tests are also shown for comparison.

The model body, boattail, and basic region, the basic configuration being a 8-deg boattail with $L/D=1$,[18,19]‡‡ are instrumented with pressure taps. The individual pressures are recorded from a series of rapid-response transducers. Combined with Schlieren photographs (and in some cases oil flow photographs), this allows the accurate determination of the external flow-jet interference pattern. In particular and as noted earlier, location of the plume-induced separation on the afterbody is a very sensitive measure of plume interference effects and of the accuracy obtained by use of the proposed modeling methodology.

Based on the earlier series of experiments conducted with air nozzles,[16,18,19] calculations were carried out according to the methodology of Sec. II to select the best-suited prototype configuration for initial Freon-22 modeling tests. The results mapped into the Freon facility performance plane are shown in Fig. 5. Based on these calculations, the air nozzle with a nominal exit Mach number of 2.5 and a conical wall angle of 10 deg was selected as the prototype (see Fig. 10a). Design conditions were chosen to allow for both design and off-design experimentation with the Freon nozzles for a typical case with plume-induced separation ($M_{L,M}=3.9$, $\theta_{L,M}=19.76$ deg, see Fig. 10b, corresponding to $p_L/p_E\,|_P=6.1$) and with emphasis on base drag no external flow separation, ($M_{L,M}=3.19$, $\theta_{L,M}=14.19$ deg, see Fig. 10c, corresponding to $p_L/P_E\,|_P=0.60$). Operating ranges for these model tests are also shown in Fig. 5.

‡‡Detailed information concerning wind tunnel operating conditions, Reynolds number ranges, and boundary layer surveys is given in Ref. 16.

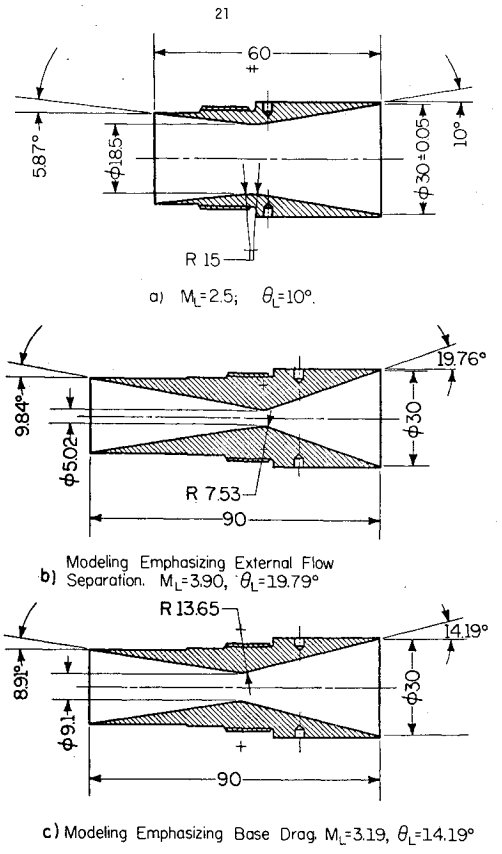

Fig. 10 Prototypes (air, $\gamma_p=1.4$) and model nozzles (Freon-22, $\gamma_M=1.16$) used in tests.

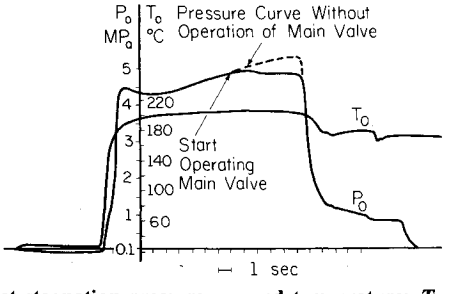

Fig. 11 Jet stagnation pressure p_{0l} and temperatures T_{0l} during a typical test run with Freon-22.

Computer calculations using the method of characteristics, following transonic flow solutions for the nozzle throat region, have been carried out confirming the validity of conical source flow approximations near the lip for both prototype and model nozzles.[13,21]

Systems Performance Tests

Shakedown tests were performed to check the temperature and pressure performance of the Freon plume simulation facility. The base pressure drag (no external flow separation) model nozzle was selected for these tests due to its lower operating pressure level requirements.

The initial tests showed that the sequence of valve opening and preheating of the lines between the Freon heater and model, referring to Fig. 6, are important to stagnation temperature performance. It was also found that stagnation pressures were not constant. Figure 11 shows the stagnation temperature and pressure recorded during a typical run. The temperature performance is seen to be satisfactory—although approximately 40-50°C lower than anticipated; however, the pressure tends to rise continually during a run. The unexpectedly high temperature loss occurs in the piping within the

tunnel and in the model itself. Methods for decreasing this loss are currently being investigated. The pressure variation is apparently caused by the acceleration of the liquid Freon in the cold portion of the system combined with its rapid vaporization as it enters the lower portion of the heated tubes. While this problem may be alleviated at lower stagnation pressures by throttling, it led to the adoption of the fast-response transducers for the pressure measurements. Combined with synchronized Schlieren photographs, the current procedure allows a range of pressure conditions to be monitored in a single run as the stagnation pressure varies.

Plume Modeling Experiments

Wake pressure ratios obtained for the two model cases, i.e., emphasizing, respectively, afterbody separation and base drag, are most appropriately interpreted in comparison to the prototype. Consequently, the test results presented below are compared on the basis of the corresponding prototype (air) pressure ratios as determined by the methods of Sec. II, Eqs. (3-8).

The agreement achieved between the prototype air plume and model Freon plume shapes based on the modeling procedure outlined in Sec. II is shown in Fig. 12. The Schlieren photos, Fig. 12, are seen to be nearly identical. A direct comparison of the essential features of the two flowfields from photo overlays shows the agreement is also satisfactory for slip-stream and plume geometries along the entire near wake region.

Shown in Fig. 13a is the experimentally determined relation

$$p_b/P_E\,|_M = f[p_{0I,M}\,(\text{MPa});\ \text{for}\ M_E=2.01,\ p_{0E}=0.1\ \text{MPa}]$$

for the model nozzle Fig. 10b. The theoretical prototype curve is found with the help of Eqs. (3-8) which yield the corresponding stagnation pressures in accordance with Fig. 13b. From these results, it can be seen that the present modeling technique allows investigations of the plume-induced separation phenomena with air at much lower nozzle-to-ambient stagnation pressure ratios than would be required for many conventional propellants as $\gamma_M > \gamma_P$ (note that in the present experimental program, the roles of model and prototype have been exchanged). It is also evident that with air as model gas, replacing the Freon in the present high-pressure gas facility, very high prototype pressure ratios can be simulated.

Interpretation of the model (Freon) experiments for predicting prototype performance (air) for both base pressure, p_B/p_E, and separation location, S/D, are shown in Figs. 14 and 15. While the model nozzles have been calculated for specific design conditions, as noted above, these comparisons made over the operating range of the tests indicate off-design applicability of the modeling procedure for each of the modeled nozzles. In particular, the base drag model nozzles, see Fig. 10c, produced excellent agreement for the entire base drag regime covering near jet-off to onset of afterbody separation.

The occurrence and location of afterbody separation was also well predicted by the appropriate nozzle, see Fig. 10b, over the range of pressures tested even though one has to expect a higher degree of sensitivity to design point selection.

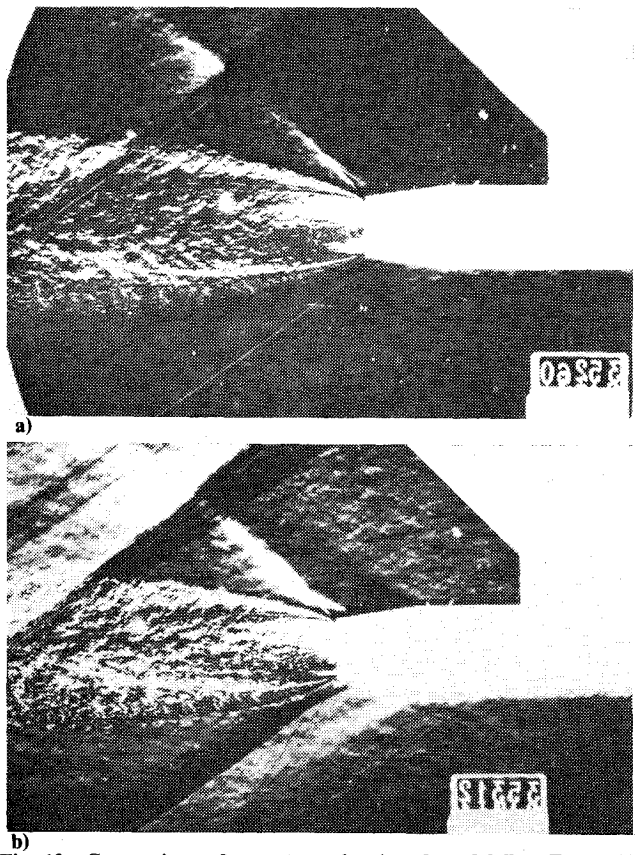

Fig. 12 Comparison of prototype air a) and model flow Freon b) configurations by Schlieren photographs.

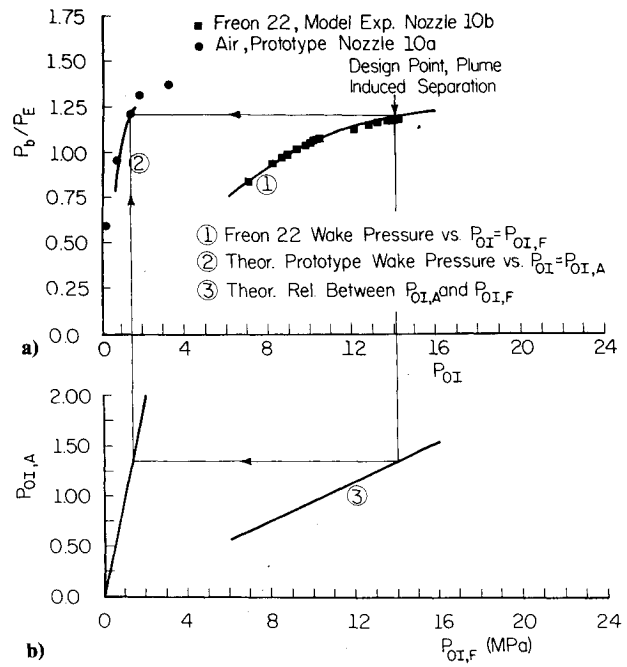

Fig. 13 Correlation between prototype (air) and model (Freon-22) test data (weak shock modeling). a) wake pressure ratio vs p_{0I}, b) P_{0I} vs $p_{0I,F}$ [Eqs. (1-3) and (9)].

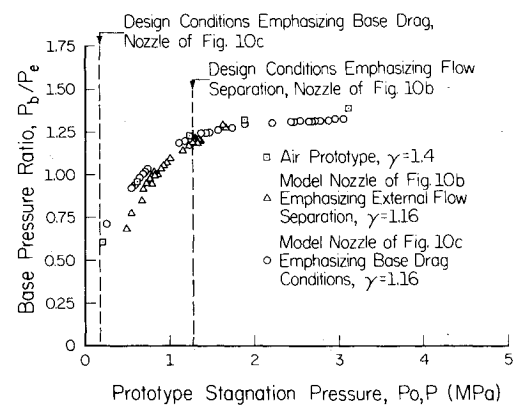

Fig. 14 Wake base pressure ratio for air (prototype) and Freon (model) tests vs prototype (air) nozzle stagnation pressure.

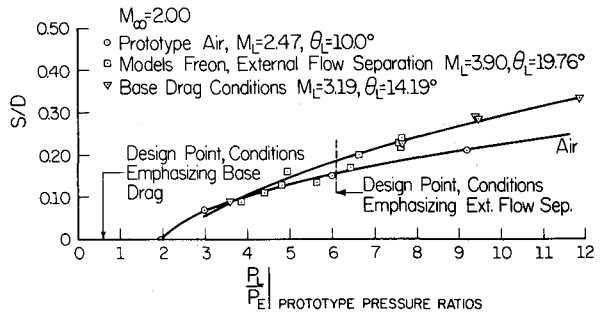

Fig. 15 Boattail separation distance for air (prototype) and Freon (model) tests vs prototype (air) nozzle lip to freestream pressure ratio.

V. Conclusions

The high-pressure, hot gas Freon jet simulation facility developed at the FFA is fully operational. It can be utilized for well-controlled jet slip-stream interference studies with a variety of gases simulating propellants. In particular, it allows the merits and the potential of plume modeling methodology suggested by Korst[12,13] to be evaluated. Equally important is the ability to critically examine the wake closure conditions for the modeling procedure, including the possible requirements for equivalent mass bleed to account in greater detail for transport phenomena across the plume boundary.

The initial tests show good agreement with anticipated facility performance. The Freon plume shapes have been found to be in close agreement with those of the corresponding air test supporting the suggested modeling methodology and design procedures. Confirmation was thus obtained that modeling of hot, low specific heat ratio propellants can be successfully accomplished by using air or nitrogen at substantially lower stagnation pressures.

Agreement between prototype and model experiments for base pressures was satisfactory not only for the design point but also for a rather wide range of off-design conditions. The more sensitive separation distance was also well correlated, however, only for a narrower range, in the vicinity of the design point. The weak shock is physically realistic for the flow near the confluence point, and this modeling scheme appears to be appropriate for plume slip-stream interactions.

Since the dynamic recompression modeling relation is not restricted to axisymmetric stream confluence geometries and as wake pressures are practically constant in case of large separation regions, the simulation methodology should remain valid for afterbodies having more complex geometries and for cases involving appreciable angles of attack, $\alpha \neq 0$.

Acknowledgment

This research program is supported jointly by the European Research Office, U.S. Army, Grant No. DA-ERO-78-G-028, The Aeronautical Research Institute of Sweden (FFA), the U.S. Army Research Office under Grant No. DAAG-29-76-G-0209 to the University of Illinois, and several Task Orders issued to H.H. Korst, Advisor to U.S.A. MIRADCOM.

References

[1] Addy, A.L., Korst, H.H., Walker, B.J., and White, R.A., "A Study of Flow Separation in the Base Region and Its Effects during Powered Flight," AGARD-CP-124, *AGARD Conference Proceedings No. 124 on Aerodynamic Drag,* Specialists' Meeting, April 10-13, 1973. (Available from NASA, Langley Field, Va. 23365, ATTN: Report Distribution and Storage Unit.)

[2] Alpinieri, L.J. and Adams, R.M., "Flow Separation due to Jet Pluming," *AIAA Journal,* Vol. 4, 1966, pp. 1865-1866.

[3] Deep, R.A., Henderson, J.H., and Brazzel, C.E., "Thrust Effects on Missile Aerodynamics," U.S. Army Missile Command, RD-TR-71-9, May 1971.

[4] Blackwell, K.L. and Hair, L.M., "Space Shuttle Afterbody Aerodynamics/Plume Simulation Data Summary," NASA Technical Paper 1384, 1978.

[5] "High Reynolds Number Research," NASA CP-2009, Oct. 27-28, 1976.

[6] Korst, H.H., Chow, W.L., and Zumwalt, G.W., "Research on Transonic and Supersonic Flow of a Real Fluid at Abrupt Increases in Cross Section (with Special Consideration of Base Drag Problems)—Final Report," University of Illinois, ME-TN-392-5, Dec. 1959.

[7] Carriere, P., Siriex, M., and Delery, J., "Methodes de Calcul des Ecoulements Turbulents Decolles en Supersonique," *Progress in Aerospace Science,* Vol. 16, No. 4, 1975, pp. 385-429.

[8] Goethert, B.H. and Barnes, L.T., "Some Studies of the Flow Pattern at the Base of Missiles with Rocket Exhaust Jets," Arnold Engineering Development Center, Tullahoma, Tenn., AEDC-TR-58-12, June 1960.

[9] Herron, R.D., "Investigation of Jet Boundary Simulation Parameters for Underexpanded Jets in a Quiescent Atmosphere," Arnold Engineering Development Center, Tullahoma, Tenn., AEDC-TR-65-6, Sept. 1968.

[10] Sims, J.L. and Blackwell, K.L., "Base Pressure Correlation Parameters," Missile and Plume Interaction Flow Fields Workshop, Redstone Arsenal, Ala., June 7-8, 1977.

[11] Johannesen, N.H. and Meyer, R.E., "Axially-Symmetrical Supersonic Flow near the Centre of an Expansion," *The Aerospace Quarterly* Vol. 2, 1950, pp. 127-42.

[12] Korst, H.H., "Approximate Determinations of Jet Contours near the Exit of Axially Symmetrical Nozzles as a Basis for Plume Modeling," U.S. Army Missile Command, TR-RD-72-14, Aug. 1972.

[13] Korst, H.H. and Deep, R.A., "Modeling of Plume Induced Interference Problems in Missile Aerodynamics," AIAA Paper No. 79036, Jan. 1979.

[14] Dods, J.B., Jr., Brownson, J.J., Kassner, D.L., Blackwell, K.L, Decker, J.P., and Roberts, B.B., "Effect of Gaseous and Solid Simulated Jet Plumes on an 040A Space Shuttle Launch Configuration at M = 1.6 to 2.2," NASA TMX-3032, April 1974.

[15] Reid, C.F., "Effects of Jet-Plume and Pressure Distributions over a Cylindrical Afterbody at Transonic Speeds," Calspan, AA-4017-W-15, W.A. T17-160, T17-170, Feb. 1979.

[16] White, R., and Agrell, J., "Boattail and Base Pressure Prediction including Flow Separation for Afterbodies with a Centered Propulsive Jet and Supersonic External Flow at Small Angles of Attack," AIAA/SAE Preprint No. 77-958, July 1977.

[17] Staff, FFA, "FFA Wind Tunnel Facilities, Part 2—Transonic-Supersonic Tunnels," The Aeronautical Research Institute of Sweden (FFA), Memorandum 93, 1969.

[18] Agrell, J., and White, R.A., "An Experimental Investigation of Supersonic Axisymmetric Flow over Boattails with a Centered Propulsive Jet," The Aeronautical Research Institute of Sweden (FFA), Technical Note AU-913, Dec. 1974.

[19] White, R.A., "The Calculation of Supersonic Axisymmetric Afterbody Flow with Jet Interference and Possible Flow Separation," The Aeronautical Research Institute of Sweden (FFA), Technical Note AU-912, 1974.

[20] Henson, V.K., Sims, J.L., and Blackwell, K.L., "Preliminary Report," Northrop Services, Inc., Report No. TN-230-1267, April 19, 1974.

[21] Nyberg, S.-E., Agrell, J., and Hevreng, T., "Investigation of Modeling Concepts for Plume-Afterbody Flow Interactions," European Research Office, U.S. Army, 1st Annual Technical Report, Feb. 1979.